Journal of Optoelectronics and Advanced Materials Vol. 6, No. 2, June 2004, p. 449 - 457

STRUCTURE AND OPTICAL PROPERTIES OF THERMALLY VACUUM EVAPORATED Sb_2O_3 THIN FILMS

N. Tigau*, V. Ciupina[a], G. Prodan[a], G. I. Rusu[b], C. Gheorghies, E. Vasile[c]

Faculty of Science, "Dunarea de Jos" University, Galati, R-6200, Romania
[a] "Ovidius" University, Constanta, R-8700, Romania
[b] Faculty of Physics, "Alexandru Ioan Cuza" University, Iasi, R-6600, Romania
[c] S.C. METAV S.A, Bucuresti, R-7200, Romania

Antimony trioxide (Sb_2O_3) thin films were prepared by thermal vacuum evaporation technique onto glass substrates kept at 20 °C and 200 °C, respectively. Films structure, grain size, morphology and roughness of surface were determined by X-ray diffraction (XRD), transmission electron microscopy (TEM), scanning electron microscopy (SEM) and atomic force microscopy (AFM). The obtained films (0.8 μm) have a face centered cubic (FCC) polycrystalline structure with the lattice constant a=11.16 Å. The optical constants (the refractive index n, the extinction coefficient k) of the films were derived from optical transmission spectra in the wavelength range 290-1200 nm, using the Swanepoel method. The analysis of the spectral dependence of the absorption coefficient α, in the intrinsic absorption region revealed the existence of an indirect allowed optical transition with energy band gap 2.75 and 2.85 eV for films deposited at substrate temperature 20 °C and 200 °C, respectively.

(Received June 9, 2003; accepted after revision January 29, 2004)

Keywords: Antimony trioxide, X-ray diffraction, Transmission electron microscopy, Scanning electron microscopy, Atomic force microscopy, Optical properties

1. Introduction

Compound of the column V-B (As, Sb, Bi) and VI-B (O, S, Se, Te) elements in the periodical table with chemical formulas $M_2^{V-B}N_3^{VI-B}$ basically have the crystal structure of antimony sulfide [1].

Group V-VI compound thin films have potential application in optoelectronic devices, photoelectrochemical devices, thermoelectric coolers, solar selective and decorative coating [2]. The increasing need for these films called for the employment of various deposition techniques such as electrodeposition [2], spray pyrolysis [3], alkaline bath chemical evaporation [4-6], dip-dry method [7], successive ionic layer adsorption and reaction method [8], microemulsion method [9], chemically vapor deposition [10] and thermal sputtering [11]. In the last few years, some experimental reports appeared on the electrical properties of oxide gasses containing Sb_2O_3 as glass formers [12,13]. The presence of Sb_2O_3 in silicate glasses leads to interesting electrical behavior at a temperature of around 300 K. Electrical conduction in these glasses below 300 K has been shown to arise owing to the hopping of a pair of electrons (bipolarons) between ion sites having different valences, i.e. Sb^{3+}-Sb^{5+} [12]. The addition of Sb_2O_3 to the binary vanadium tellurite gasses changes the nature of hopping from non-adiabatic to adiabatic [13].

As part of a study of the homologous series of compound of Sb with group VI elements we have investigated the effect of substrate temperature of antimony trioxide (Sb_2O_3) thin films on

*Corresponding author: ntigau@ugal.ro

structural and optical properties. Sb_2O_3 has two crystalline modifications: orthorhombic Pccn, D_{2h}^{10} (valentinite) and cubic Fd3m, O_h^7 (senarmontite) [14]. Both forms of Sb_2O_3 exist as natural materials, the former as a valentinite and the latter as senarmontite.

In this paper we report the preparation of cubic Sb_2O_3 thin films using the thermal vacuum evaporation technique at different substrate temperatures. A detailed study of the structural and optical properties has been carried out for these films.

2. Experimental

Antimony trioxide (Sb_2O_3) thin films were deposited onto microscope cover glass substrate in a thermal vacuum evaporation system ($p=5\times10^{-5}$ torr) using a starting material of polycrystalline powder of Sb_2O_3 with a purity of 99.99% (Merck). The temperature of the evaporation source was kept constant at melting point of Sb_2O_3 (656 ^oC). The Sb_2O_3 films were deposited at substrate temperatures 20 ^oC and 200 ^oC to an accuracy of ±2 ^0C with a deposition rate 60 Å/s by controlling the filament current and final thickness of approximately 0.80 μm. The thickness of the films was measured by interferometric method [15] using an MII-4 type Linnik microscope.

The surface micro roughness of the films was measured by using a Digital Instruments Nanoscope III atomic force microscope (AFM).

Investigation of the microstructure was carried out using an X-ray diffractometer (Dron 3) and a Philips CM-120 transmission electron microscope (TEM) operated at 100 kV with a calibrated resolution 0.4 nm. X-ray diffraction (XRD) patterns were recorded automatically using CuK_α radiation (λ=1.5418 Å) with Ni filter operated at 32 kV and 22 mA with scanning rate of 0.5 deg/min in the scanning angular range from 10 to 60^o.

Optical properties of Sb_2O_3 thin films were studied using transmittance spectra obtained from a double-beam spectrophotometer (Specord UV-VIS M-40) in the range of wavelengths from 300-1200 nm. The effect of substrate is compensated experimentally and the optical transmission of the glass substrate. The spectra were measured at room temperature in clean air.

3. Results and discussion

The analysis of the XRD and TEM patterns represented in Fig. 1 and Fig. 2, respectively, for the studied samples revealed a strong dependence of structural characteristics of the films on the substrate temperature. Careful analysis of X-ray diffraction pattern (Fig. 1) indicates the polycrystalline nature of cubic FCC unit cell with lattice parameter a=11.16 Å, witch are in good agreement with the earlier data [14]. This appears to be the only phase present in the films.

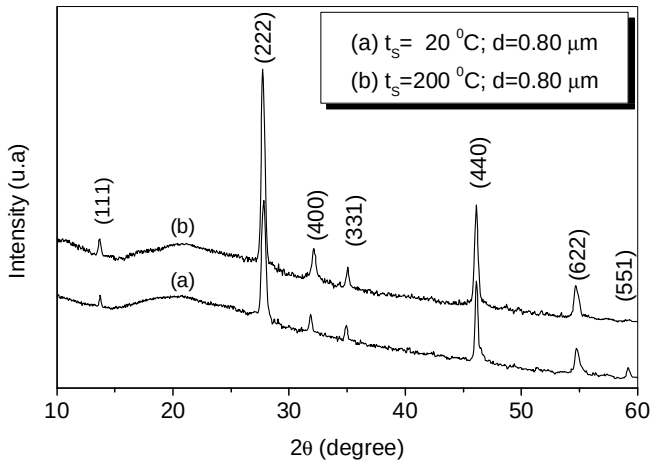

Fig. 1. XRD pattern of Sb_2O_3 thin film deposited at (a) 20 ^oC and (b) 200 ^oC.

The crystallites are preferentially oriented with the (222) planes parallel to the substrate. As the substrate temperature was increased from 20 to 200 ^oC the intensity of the peak corresponding to the (222) planes increased. At substrate temperature t_S=20 ^oC the small peak corresponding to the (551) plane disappeared but the intensity of the peak corresponding to the (440) plane increased.

The interplanar distances ($d_{hk\ell}$) of the polycrystalline structure of the Sb_2O_3 thin films were calculated by means of following expression:

$$d_{hk\ell} = \frac{\lambda L}{R} \tag{1}$$

where λ=0.037 Å, is the electron wavelength at 100 kV, L is the camera length of the TEM and R is radius of the rings from the electron diffraction pattern (Fig. 2a and 2b).

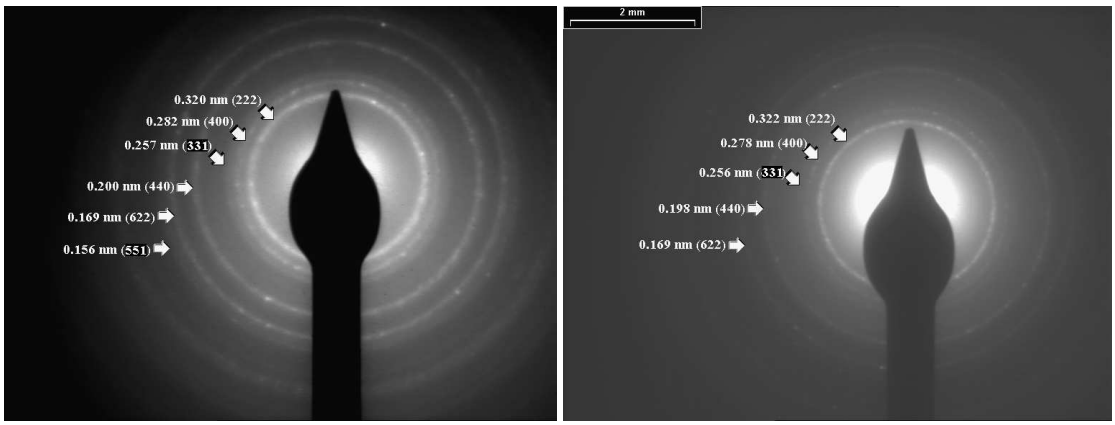

(a) (b)

Fig. 2. TEM pattern of Sb_2O_3 thin films deposited at (a) 20 ^oC and (b) 200 ^oC.

Table 1 shows the calculated interplanar distances and the standard values for the cubic FCC structure of Sb_2O_3.

Table 1. The interplanar distances ($d_{hk\ell}$) for Sb_2O_3 thin films.

hkl	$d_{hk\ell}$ *(nm) calculated*		$d_{hk\ell}$ *(nm)*
	t_S=20 ^0C	t_S=200 ^0C	*standard*
(111)	0.644	0.645	0.643
(222)	0.320	0.322	0.321
(400)	0.282	0.278	0.278
(331)	0.257	0.256	0.214
(440)	0.200	0.198	0.197
(622)	0.169	0.169	0.168
(511)	0.156	-	0.156

Figs. 3a and 3b show scanning electron micrographs (SEM) of the Sb_2O_3 thin films deposited at substrate temperature t_S=20 ^oC and t_S=200 ^oC, respectively. The SEM investigations confirm the polycrystalline structure of the Sb_2O_3 thin films. The grains have small dimensions and a uniform their distribution on the whole substrate surface evinced. A slight increase in the crystallite size with increasing substrate temperature was observed for the investigated samples.

The grain size calculated from the intercept method according to [16]:

$$D = \frac{1.5\,\ell}{Nm} \tag{2}$$

where m is the micrograph magnification, ℓ is the line length on the micrograph, N is the number of grains crossed by the line and 1.5 is a shape parameter, assuming spherical grains.

The average grain size was found to increases from 48 to 92 nm as the substrate temperature was increases from 20 ^{o}C to 200 ^{o}C

This observation is confirmed by high-resolution TEM observation (HRTEM) in which the different fringe patterns, corresponding to a different orientation of the grains, show more accurately the extension of each single grain (Fig. 4a and 4b).

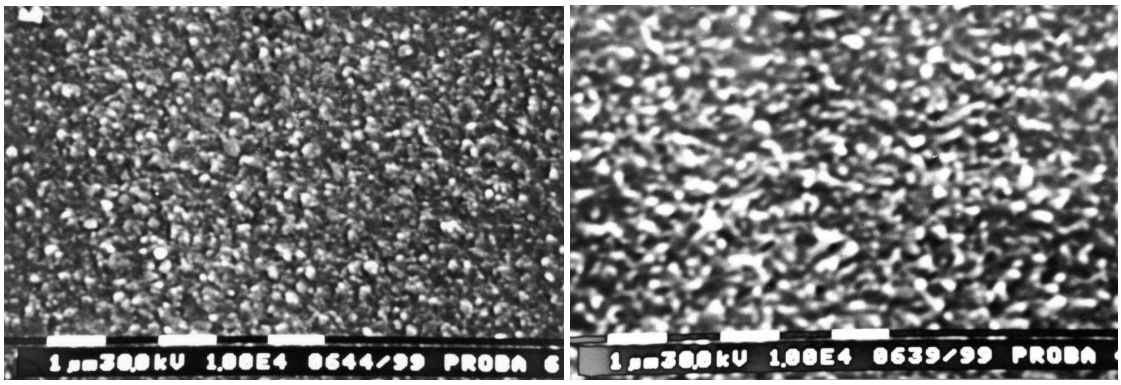

(a) (b)

Fig. 3. SEM micrographs of Sb_2O_3 thin films deposited at (a) 20 ^{o}C and (b) 200 ^{o}C.

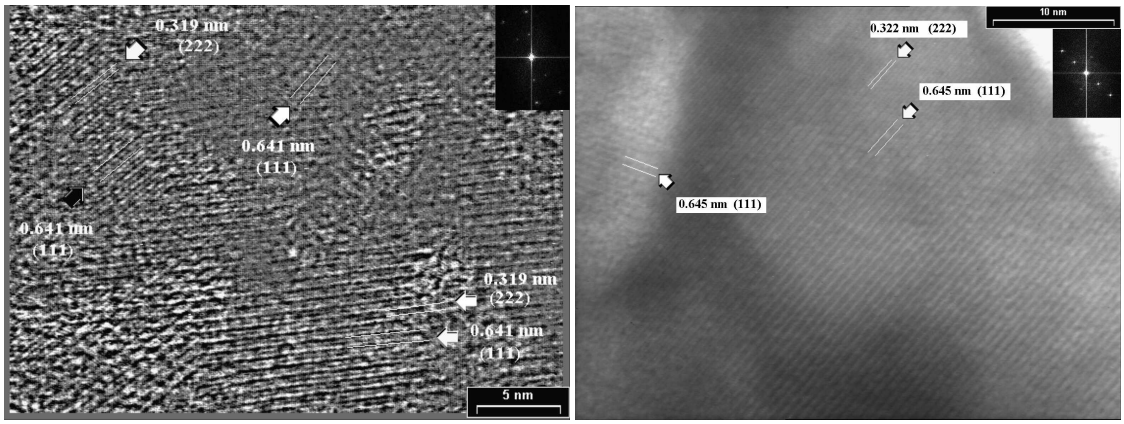

(a) (b)

Fig. 4. HRTEM image of Sb_2O_3 thin films deposited at (a) 20 ^{o}C and (b) 200 ^{o}C.

Atomic force microscopy (AFM) was used to examine the surface morphology of Sb_2O_3 thin films. Figs. 5a and 5b shows the AFM micrographs (5×5 μm^2) for studied samples.

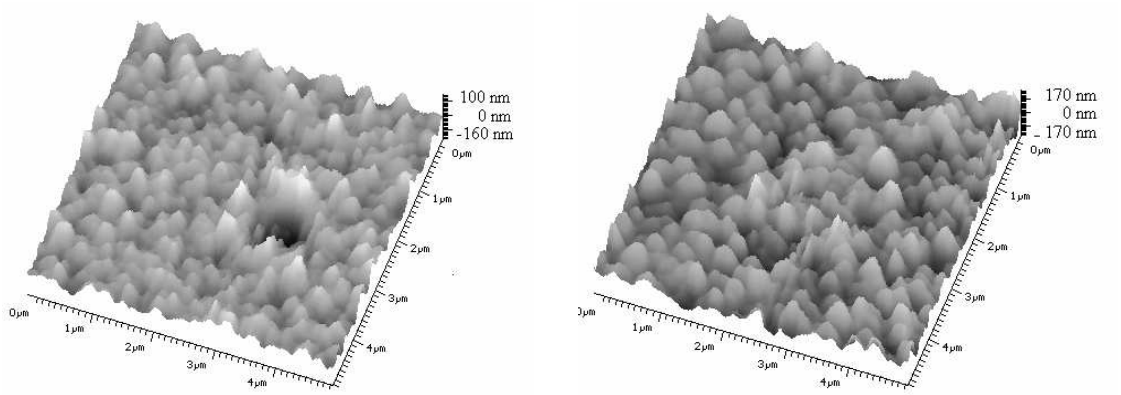

Fig. 5. AFM micrographs (5×5 μm^2) of Sb_2O_3 thin films deposited at (a) 20 ^{o}C and (b) 200 ^{o}C.

The grain-like morphology can be seen in both samples and the topography of samples was not changed as the substrate temperature increases from 20 to 200 ^{o}C. However, the average roughness decrease from 47 to 34 nm as the substrate temperature increases from 20 to 200 ^{o}C. It is generally known that the annealing of polycrystalline films results in reduction of surface roughness [17]. The average roughness were calculated by the arithmetic mean of N deviation in height (Z_i) from the profile mean value (Z_m) [18]:

$$H_a = \frac{1}{N}\sum_{i=1}^{N}\left|Z_m - Z_i\right| \tag{3}$$

The optical transmission through the films was measured using a double-beam spectrophotometer. Fig. 6 shows the measured transmission spectra for Sb_2O_3 thin films prepared at different substrate temperature (20 ^{o}C and 200 ^{o}C). From this figure it is inferred that the average transmission over the 900-1200 nm range exceeds 80%. The transmission spectrum of these films shows two zones, one up to the absorption edge and second beyond it. Below the absorption edge it can be considered [19] as a non-absorbing film and non-absorbing substrate due to the small value of absorption in this wavelength range. Above the band edge, it can be considered as a thin absorbing film on a thick non-absorbing substrate at is well known that this region exhibits a series of maxima and minima due to interference [20]. The original relation for calculating the value of the absorption coefficient from measured transmittance values for semiconducting thin films was given by Manifacier *et al*. [21] and later modification were made by Neumann *et al*. [19] and Swanepoel [22].

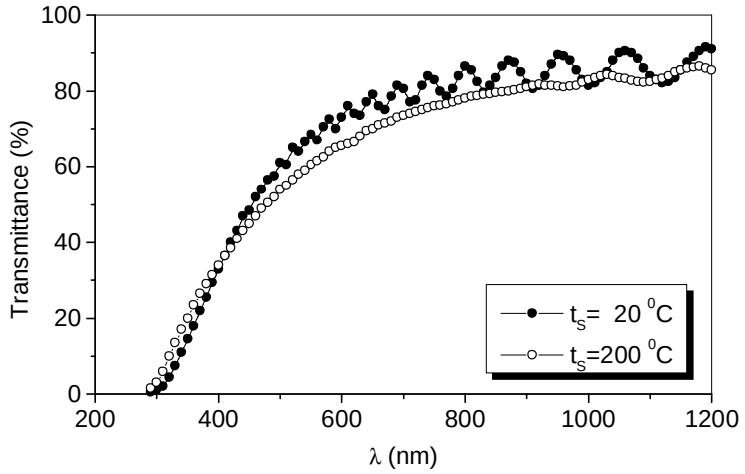

Fig. 6. The dependence of transmittance of the Sb_2O_3 thin films on the wavelength.

The optical parameters such as refractive index (n), absorption coefficient (α) and extinction coefficient (k) were determined from transmission spectrum using the Swanepoel`s method [22-25].

The refractive index (Fig. 7) was found from:

$$n=[N+(N^2-n_s^2)^{1/2}]^{1/2} \tag{4}$$

with:

$$N=\frac{n_s^2+1}{2}+2n_s\frac{T_M-T_m}{T_M T_m} \tag{5}$$

where n_S = 1.50 is the refractive index of the substrate. T_M and T_m are the maximum and minimum values respectively of the transmission spectrum.

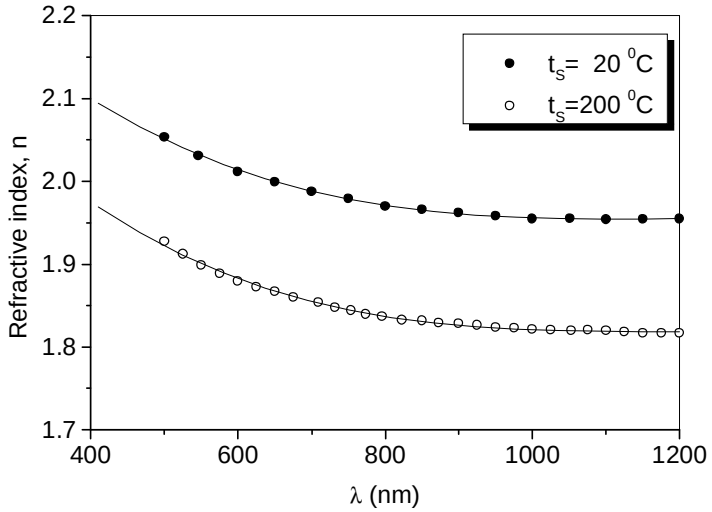

Fig. 7. Refractive index of Sb_2O_3 thin films as a function of wavelength.

The absorption coefficient (α) of the thin films can be calculated by the expression:

$$\alpha=-\frac{\ln x}{d} \tag{6}$$

In the region of weak and medium absorption parameter x were calculation from the relation:

$$x=\frac{E_M-[E_M^2-(n^2-1)^3(n^2-n_s^4)]^{1/2}}{(n-1)^3(n-n_s^2)} \tag{7}$$

$$E_M=\frac{8n^2n_s}{T_M}+(n^2-1)(n^2-n_s^2) \tag{8}$$

In the region of strong absorption the values of x can be calculated using the relation:

$$x\cong\frac{(n+1)^3(n+n_s^2)}{16\,n^2n_s}T_0 \tag{9}$$

where T_0 is the values of transmission in region of strong absorption.

Once $\alpha(\lambda)$ is known, extinction coefficient $k(\lambda)$ can be calculated by the expression:

$$k = \frac{\alpha\lambda}{4\pi} \tag{10}$$

witch completes the calculation of the optical constants.

According to Fig. 7 the refractive index of the two thin films deposited on a substrate having a temperature of 20 ^{o}C and 200 ^{o}C, respectively, presents a normal dispersion on the whole wavelength range, but it is strongly influenced of substrate temperature.

Figs. 8 and 9 represent the dependence $\alpha(h\nu)$ and $k(\lambda)$ for Sb_2O_3 thin films deposited at different substrate temperature. From these figures shown that the absorption coefficient (α) and extinction coefficient (k) were slightly affected by substrate temperature. However, the absorption coefficient is slightly affected by the change of substrate temperature at lower energy values, while the change is observed at higher energy values.

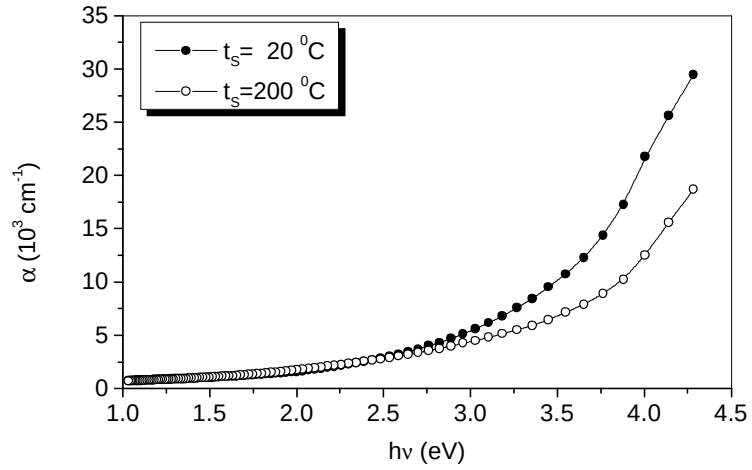

Fig. 8. Variation of absorption coefficient with photon energy for Sb_2O_3 thin films.

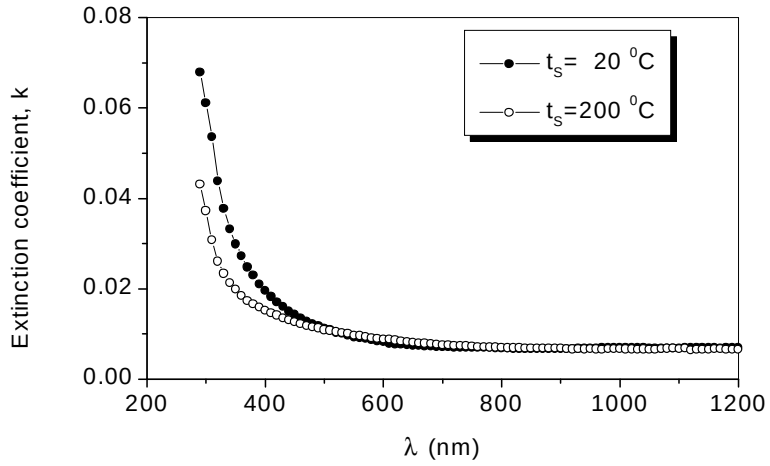

Fig. 9. Variation of extinction coefficient for Sb_2O_3 thin films on the wavelength.

The intrinsic absorption edge was examined using the equation [26-29]:

$$\alpha h\nu = A(h\nu - E_g)^r \tag{11}$$

where r= 1/2 and 2 for direct and indirect allowed optical transition respectively and A is a characteristic parameter, independent on photon energy. In an order to know whether there is one type of optical transition or more that can exist in Sb_2O_3 thin polycrystalline films, a graphical representation of $(\alpha h\nu)^{1/r} = f(h\nu)$ for Sb_2O_3 thin films prepared at different substrate temperature [27]. Figs. 10 and 11 represent both $(\alpha h\nu)^{1/2} = f(h\nu)$ and $(\alpha h\nu)^2 = f(h\nu)$ for Sb_2O_3 thin films deposited at substrate temperature 20 ^oC and 200 ^oC, respectively. It is obvious that the second relation yields a straight line indicating the existence of indirect optical transition with an energy band gap $E_g = 2.75$ eV for film deposited at 20 ^oC and $E_g = 2.85$ eV for film deposited at 200 ^oC. The values of energy band gap, E_g, have been determined by extrapolating the linear portions of the respective curves to $(\alpha h\nu)^{1/2} = 0$. These values are in good agreement with the values reported for crystals of cubic antimony trioxide [14,30].

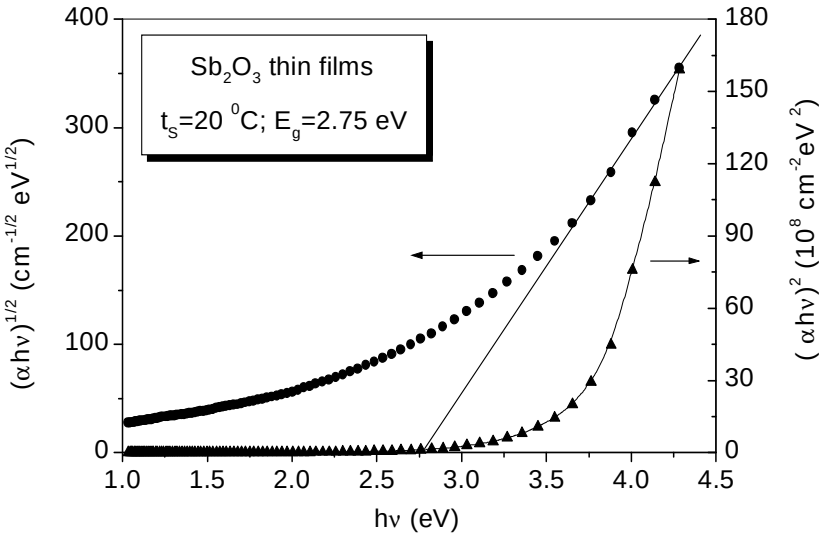

Fig. 10. The dependence of $(\alpha h\nu)^{1/2}$ and $(\alpha h\nu)^2$ on photon energy $(h\nu)$ for the Sb_2O_3 thin films deposited at 20 ^oC.

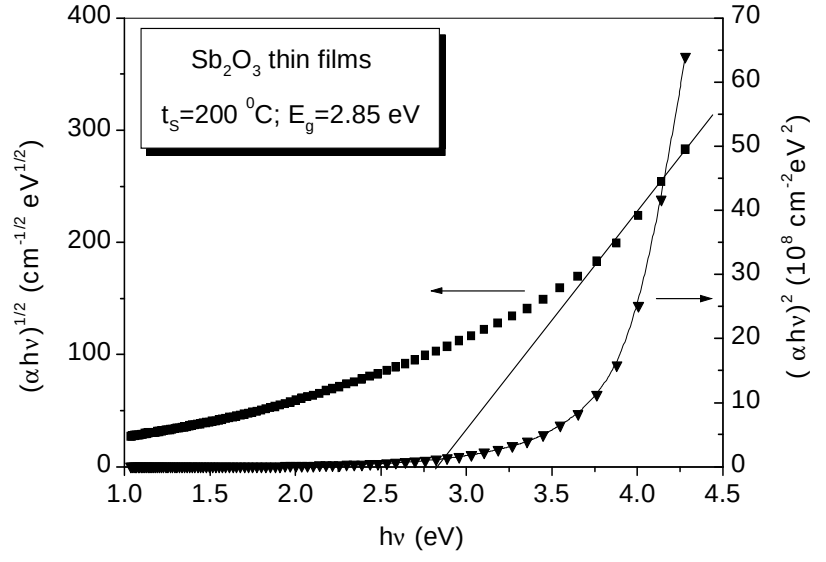

Fig. 10. The dependence of $(\alpha h\nu)^{1/2}$ and $(\alpha h\nu)^2$ on photon energy $(h\nu)$ for the Sb_2O_3 thin films deposited at 200 ^oC.

5. Conclusions

In this study, the influence of substrate temperature on the structural and optical properties of Sb_2O_3 thin films was investigated thus completing the data obtained in [31]. The XRD and TEM study reveals that these films, deposited at substrate temperature: 20 ^oC and 200 ^oC, have the polycrystalline nature corresponding to an FCC phase with lattice parameter a=11.16 Å.

As the substrate temperature increases from 20 ^oC to 200 ^oC, the average grain size increases from 48 to 92 nm and the average roughness decrease 47 from to 34 nm. Consequently, the optical band gap corresponding of the indirect transition increases from 2.75 to 2.85 eV as the substrate temperature varies from 20 to 200 ^oC.

References

[1] C. Kaito, T. Fujita, T. Kimura, K. Hanamoto, N. Suzuki, S. Kimura, Y. Saito, Thin Solid Films **312**, 93 (1998).
[2] N. S. Yesugade, C. D. Lokhande, C. H. Bhosale, Thin Solid Films **263**, 145 (1995).
[3] C. H. Bhosale, M. D. Uplane, P. S. Patil, C. D. Lokhande, Thin Solid Films **248**, 137 (1994).
[4] J. Desai, C. D. Lokhande, Thin Solid Films **237**, 29 (1994).
[5] I. K. El Zawawi, A. Abdel-Moez, F. S. Terra, M. Mounir, Thin Solid Films **324**, 300 (1998).
[6] I. K. El Zawawi, A. Abdel-Moez, F. S. Terra, M. Mounir, Fizica **A7**(3), 97 (1998)
[7] B. B. Nayak, H. N. Acharya, T. K. Chandhuri, G. B. Mitra, Thin Solid Films **92**, 304 (1982).
[8] B. R. Sankapal, R. S. Mane, C. D. Lokhande, Journal of Materials Science Letters **18**, 1453 (1999).
[9] Lin Guo, Z. Wu, T. Liu, W. Wang, H. Zhu, Chemical Physics Letters **318,** 49 (2000).
[10] A. M. Salem, M. Soliman Selim, J. Phys.D: Appl. Phys. **34**, 12 (2001).
[11] C. Gheorghies, L. Gheorghies, J. Optoelectron. Adv. Mater. **4**, 979 (2002).
[12] A. Datta, A. K. Giri, D. Chakravorty, J. Phys: Condensed Matter **4**, 1783 (1992).
[13] G. Ghosh, J. Phys: Condensed Matter **5**, 4483 (1993).
[14] C. Wood, B. Van Pelt, A. Dwight, Physica Status Solidi **(b) 54**, 701 (1972).
[15] K. L. Chopra, Thin Solid Fenomena, McGraw-Hill, New York, 1969
[16] Y. Wada, S. Nishimatsu, J. Electrochem. Soc. **125**, 1499 (1978).
[17] A. H. Jayatissa, Semicond. Sci. Technol. **18**, L27 (2003).
[18] A. M. Chaparro, C Maffiotte, M. T. Gutierrez, J. Herrero, Thin Solid Films **358**, 22 (2000).
[19] H. Neumann, W. Horing, E. Reccins, H. Sobotta, B. Schumann, G. Kuhu, Thin Solid Films **61**, 13 (1979).
[20] K. C. Sharma, J. C. Garg, J. Phys. D: Appl. Phys. **23**, 1411 (1990).
[21] J. C. Manifacier, J. Gasiot, J. P. Fillard, Phys. E: Appl. Phys. **9**, 1002 (1976).
[22] R. J. Swanepoel J. Phys. E. Sci. Instrum. **16**, 1214 (1983).
[23] Li-Jian Meng, M. Andritshky, M. P. dos Santos, Thin Solid Films **223**, 242 (1993).
[24] E. Marquez, J. B. Ramirez-Malo, P. Villares, R. Jimenez-Garay, R. J. Swanepoel, Thin Solid Films **254**, 83 (1993).
[25] N. Tigau, G. I. Rusu, C. Gheorghies, J. Optoelectron. Adv. Mater. **4**, 943 (2002)
[26] J. Tauc (ed.), Amorphous and Liquid Semiconductors, North-Holland, Amsterdam, 1974.
[27] H. S. Soliman, D. Abdel-Hady, E. Ibrahim, J. Phys: Condensed Matter **10**, 847 (1998).
[28] R. P. Sharma, K. C. Sharma, J. C. Garg, J. Phys. D: Appl. Phys. **24**, 2084 (1991).
[29] G. Venkata Rao, G. Hema Chandra, P. Sreedhara Reddy, O. M. Hussain, K. T. Ramakrishna Reddy, S. Uthanna, J. Optoelectron. Adv. Mater. **2**, 387 (2002)
[30] B. Wolffing, Z. Hurych, Physica Status Solidi **(a) 16**, K161 (1973).
[31] N. Tigau, V. Ciupina, G. Prodan, G. I. Rusu, C. Gheorghies, E. Vasile, J. Optoelectron. Adv. Mater. **5**(4), 907 (2003).